Pairing of spinless fermions in two dimensions

Jian Ping Lu
Loomis Laboratory of Physics, University of Illinois at Urbana-Champaign, Urbana, Illinois 61801

W. Barford
Department of Physics, University of Sheffield, Sheffield S3 7RH, United Kingdom
(Received 17 January 1991; revised manuscript received 10 May 1991)

We study the real-space pairing instability of spinless fermions on a two-dimensional square lattice with short-range attractive interactions. Various symmetries of the pairing order parameter are considered. It is found that in both nonflux and flux phases the most stable pairing state is chiral and anisotropic. It breaks both the parity and the time-reversal symmetries. The quasiparticle excitation has a minimum gap which could be much smaller than its average over the Fermi surface. The temperature dependence of the order parameter and the critical magnetic field are found to be similar to those of the classical BCS solutions. A possible connection with the high-temperature superconductivity is discussed.

The problem of strongly correlated electrons confined to two dimensions has been of considerable interest in the last few years, in part due to the general belief that the essential physics of the high-T_c superconductivity lies within such a problem.[1] One model which has been extensively studied is the so-called t-J model which describes both the spin and charge dynamics in the strong-coupling limit.[2-4] Various effective Hamiltonians and mean-field schemes have been introduced to study the ground state and the low-energy excitations.[3-5]

In our recent work[6] we used the semiclassical approximation for the spin degrees of freedom to study the possible ground state of the charge (fermion) dynamics. In such an approach the effects of the spin dynamics on the charge movement are twofold. First, it introduces a gauge potential into the charge kinematics which in general can break both the time-reversal and parity symmetries. Secondly, an attractive interaction between holes on nearest-neighbor sites is induced. Such an interaction naturally leads to the real-space pairing instability which gives rise to a superconducting phase transition. Similarly in the large-N expansion studies of the generalized t-J model[7,8] and in variational calculations,[9] it is found that there is an effective attractive interaction between the spinless fermions which leads to the superconducting instabilities. In this paper we study such a superconducting state and the related physical properties.

We start with the effective Hamiltonian for spinless fermions in 2D with nearest-neighbor attractive interactions

$$H=\sum_{i,j} t_{ij} f_i^\dagger f_j + \text{H.c.} + \sum_{i,j} V_{ij} f_i^\dagger f_i f_j^\dagger f_j \ , \tag{1}$$

where $t_{ij}=|t_{ij}|e^{i\phi_{ij}}$ with ϕ_{ij} the gauge potential across the link $\langle ij \rangle$ and $f_i^\dagger$ creates a spinless fermion on site i. In general both the hopping amplitude $|t_{ij}|$ and the interaction V_{ij} are nonuniform. However for simplicity we will consider the uniform case, $|t_{ij}|=t$ and $V_{ij}=-V$, only. The Hamiltonian (1) is identical to the t-J Hamiltonian in the frozen spin limit up to a constant.[6] It is the simplest effective Hamiltonian which contains the essential physics in the superconducting state and is consistent with earlier studies. The gauge potential ϕ_{ij} is due to the coherent hopping of the spin in a strongly correlated spin background. The gauge invariant quantity is the total flux piercing a plaquette $\Phi=\sum_{i,j\in p}\phi_{ij}$.

Of the various spin configurations which have been studied the flux phases, which have a nonzero Φ, are of particular interest. In studying the phase diagram of the t-J model in the frozen-spin approximation we introduced a class of generalized staggered-flux phases[6] (GSFP) which are classified by the size of the unit cell, q. The $q=2$ GSFP is identical to that of the uniform flux phase when $\Phi=\pi$. In this paper we will limit ourselves to pairing in the (nonflux) tight-binding phase and the simple staggered-flux phase (namely the $q=2$ GSFP) only. The results of the superconducting gap, T_c, and the related thermodynamic properties will be discussed. In addition the various symmetries of the order parameter which are allowed will be explored.

To consider the possible real space pairing we introduce the following pairing order parameters:

$$\begin{aligned} &\Delta_{+\hat{x}}=V\langle f_i f_{i+\hat{x}}\rangle, \quad \Delta_{-\hat{x}}=V\langle f_i f_{i-\hat{x}}\rangle \ , \\ &\Delta_{+\hat{y}}=V\langle f_i f_{i+\hat{y}}\rangle, \quad \Delta_{-\hat{y}}=V\langle f_i f_{i-\hat{y}}\rangle \ . \end{aligned} \tag{2}$$

We assume that the order parameters have the translational symmetry of the lattice. In the $q=2$ flux phase the

unit cell is doubled, namely i and $i+\hat{x}$ belong to two distinct sublattices A and B (Fig. 1). Hence, in general, all four order parameters defined above are independent. The relative phases of these order parameter, as will be seen later, lead to different symmetries.

The four-fermion interaction term in the Hamiltonian (1) is decoupled using the order parameters defined, for example,

$$Vf_{i+\hat{x}}^{\dagger}f_i^{\dagger}f_if_{i+\hat{x}}=f_{i+\hat{x}}^{\dagger}f_i^{\dagger}\Delta_{+\hat{x}}+\Delta_{+\hat{x}}^{\dagger}f_if_{i+\hat{x}}-\frac{\Delta_{+\hat{x}}^{\dagger}\Delta_{+\hat{x}}}{V} . \tag{3}$$

This leads to the bilinear Hamiltonian

$$\begin{aligned}H=&\sum_{i\in A}\{[(\tilde{t}A_i^{\dagger}B_{i+\hat{x}}+\tilde{t}A_i^{\dagger}B_{i-\hat{x}}+\tilde{t}^{*}A_i^{\dagger}B_{i+\hat{y}}+\tilde{t}^{*}A_i^{\dagger}B_{i-\hat{y}})+\text{H.c.}]\\&+[(\Delta_{+\hat{x}}A_i^{\dagger}B_{i+\hat{x}}^{\dagger}+\Delta_{-\hat{x}}A_i^{\dagger}B_{i-\hat{x}}^{\dagger}+\Delta_{+\hat{y}}A_i^{\dagger}B_{i+\hat{y}}^{\dagger}+\Delta_{-\hat{y}}A_i^{\dagger}B_{i-\hat{y}}^{\dagger})+\text{H.c.}]\}\\&+\sum_{i\in A}\frac{1}{V}(\Delta_{+\hat{x}}\Delta_{+\hat{x}}^{\dagger}+\Delta_{-\hat{x}}\Delta_{-\hat{x}}^{\dagger}+\Delta_{+\hat{y}}\Delta_{+\hat{y}}^{\dagger}+\Delta_{-\hat{y}}\Delta_{-\hat{y}}^{\dagger}) ,\end{aligned} \tag{4}$$

where we have introduced the operators $A_i=f_i$ ($i\in A$) and $B_j=f_j$ ($j\in B$) to distinguish fermions on sublattices A and B, respectively. Also a symmetric gauge has been chosen such that $\tilde{t}=te^{i\Phi/4}$ with Φ being the flux through a plaquette (Fig. 1).

Since the mean-field Hamiltonian (4) no longer commutes with the number operator, it is convenient to work within the grand-canonical ensemble. Hence, defining $\tilde{H}=H-\mu\sum_i A_i^{\dagger}A_i-\mu\sum_j B_j^{\dagger}B_j$, and taking the half-space Fourier representation, we have

$$\tilde{H}=\sum_{k_x>k_y}\Psi^{\dagger}\begin{bmatrix}-\mu & \gamma(\mathbf{k}) & 0 & \Delta(\mathbf{k})\\ \gamma^{*}(\mathbf{k}) & -\mu & -\Delta(-\mathbf{k}) & 0\\ 0 & -\Delta^{\dagger}(-\mathbf{k}) & \mu & -\gamma^{*}(-\mathbf{k})\\ \Delta^{\dagger}(\mathbf{k}) & 0 & -\gamma(-\mathbf{k}) & \mu\end{bmatrix}\Psi+E_0 , \tag{5}$$

where

$$\begin{aligned}&\gamma(\mathbf{k})=2t[\cos(k_x)e^{i\Phi/4}+\cos(k_y)e^{-i\Phi/4}] , \quad \Delta(\mathbf{k})=\Delta_{+\hat{x}}e^{ik_x}+\Delta_{-\hat{x}}e^{-ik_x}+\Delta_{+\hat{y}}e^{ik_y}+\Delta_{-\hat{y}}e^{-ik_y} ,\\&E_0=\sum_{\delta=\pm\hat{x},\pm\hat{y}}\frac{N}{V}\Delta_{\delta}^{\dagger}\Delta_{\delta}+\sum_{k_x>k_y}[\gamma(-\mathbf{k})+\gamma^{*}(-\mathbf{k})+\Delta(-\mathbf{k})+\Delta^{*}(-\mathbf{k})-2\mu] ,\end{aligned} \tag{6}$$

N is the number of unit cells, and we have defined the vector $\Psi^{\dagger}$ as

$$\Psi^{\dagger}=(A_{\mathbf{k}}^{\dagger},B_{\mathbf{k}}^{\dagger},A_{-\mathbf{k}},B_{-\mathbf{k}}) . \tag{7}$$

The Hamiltonian (5) can be diagonalized to produce four eigenvalues

$$\begin{aligned}&E_{1,2}=\{\tfrac{1}{2}[\mu^2+2|\gamma|^2+|\Delta(\mathbf{k})|^2+|\Delta(-\mathbf{k})|^2\mp\sqrt{16\mu^2|\gamma|^2+[|\Delta(-\mathbf{k})|^2-|\Delta(\mathbf{k})|^2]^2+4|\Delta(-\mathbf{k})+\Delta(\mathbf{k})|^2|\gamma|^2}]\}^{1/2} ,\\&E_{3,4}=-E_{1,2} ,\end{aligned} \tag{8}$$

and corresponding eigenfunctions

$$\begin{bmatrix}\eta_1(\mathbf{k})\\ \eta_2(\mathbf{k})\\ \eta_1^{\dagger}(-\mathbf{k})\\ \eta_2^{\dagger}(-\mathbf{k})\end{bmatrix}=\begin{bmatrix}u_{11}^{*}(\mathbf{k}) & u_{12}^{*}(\mathbf{k}) & v_{11}^{*}(\mathbf{k}) & v_{12}^{*}(\mathbf{k})\\ u_{12}^{*}(\mathbf{k}) & u_{22}^{*}(\mathbf{k}) & v_{12}^{*}(\mathbf{k}) & v_{22}^{*}(\mathbf{k})\\ v_{11}(-\mathbf{k}) & v_{12}(-\mathbf{k}) & u_{11}(-\mathbf{k}) & u_{12}(-\mathbf{k})\\ v_{21}(-\mathbf{k}) & v_{22}(-\mathbf{k}) & u_{21}(-\mathbf{k}) & u_{22}(-\mathbf{k})\end{bmatrix}\begin{bmatrix}A_{\mathbf{k}}\\ B_{\mathbf{k}}\\ A_{-\mathbf{k}}^{\dagger}\\ B_{-\mathbf{k}}^{\dagger}\end{bmatrix} \tag{9}$$

which define the coherence factors u's and v's. The order parameters and the chemical potential are determined from the self-consistent equation (2) and the constraint $N^{-1}\sum_{\mathbf{k}}A_{\mathbf{k}}^{\dagger}A_{\mathbf{k}}=N^{-1}\sum_{\mathbf{k}}B_{\mathbf{k}}^{\dagger}B_{\mathbf{k}}=\delta$, where δ is the number of the fermions per lattice site.

Before we present the numerical results, let us examine the possible symmetries of the order parameters. As we pointed out, the order parameters defined in Eq. (2) are in general all independent. We will assume that the magnitude of all the order parameters is the same. This leads to the following six possibilities which are compatible with the symmetries of the square lattice:[10]

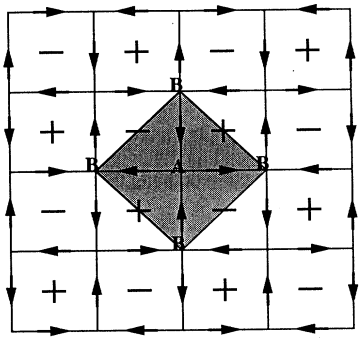

FIG. 1. The square lattice. Arrows on the bond indicate that hopping along the direction carries a phase $e^{i\Phi/4}$. The flux through a plaquette is $\Phi=\pi$.

$$
\begin{aligned}
&\text{A: } \Delta_{+\hat{x}}=-\Delta_{-\hat{x}},\ \Delta_{+\hat{y}}=-\Delta_{-\hat{y}},\ \Delta_{+\hat{y}}=\Delta_{+\hat{x}}\ ,\\
&\quad \Delta(\mathbf{k})=i2\Delta_0[\sin(k_x)+\sin(k_y)]\ ,\\
&\text{B: } \Delta_{+\hat{x}}=-\Delta_{-\hat{x}},\ \Delta_{+\hat{y}}=-\Delta_{-\hat{y}},\ \Delta_{+\hat{y}}=-\Delta_{+\hat{x}}\ ,\\
&\quad \Delta(\mathbf{k})=i2\Delta_0[\sin(k_x)-\sin(k_y)]\ ;\\
&\text{C: } \Delta_{+\hat{x}}=-\Delta_{-\hat{x}},\ \Delta_{+\hat{y}}=-\Delta_{-\hat{y}},\ \Delta_{+\hat{y}}=e^{i\pi/2}\Delta_{+\hat{x}}\ ,\\
&\quad \Delta(\mathbf{k})=i2\Delta_0[\sin(k_x)+i\sin(k_y)]\ ;\\
&\text{D: } \Delta_{+\hat{x}}=\Delta_{-\hat{x}},\ \Delta_{+\hat{y}}=\Delta_{-\hat{y}},\ \Delta_{+\hat{y}}=\Delta_{+\hat{x}}\ ,\\
&\quad \Delta(\mathbf{k})=2\Delta_0[\cos(k_x)+\cos(k_y)]\ ;\\
&\text{E: } \Delta_{-\hat{x}}=\Delta_{-\hat{x}},\ \Delta_{+\hat{y}}=\Delta_{-\hat{y}},\ \Delta_{+\hat{y}}=-\Delta_{+\hat{x}}\ ,\\
&\quad \Delta(\mathbf{k})=2\Delta_0[\cos(k_x)-\cos(k_y)]\ ;\\
&\text{F: } \Delta_{+\hat{x}}=\Delta_{-\hat{x}},\ \Delta_{+\hat{y}}=\Delta_{-\hat{y}},\ \Delta_{+\hat{y}}=e^{i\pi/2}\Delta_{+\hat{x}}\ ,\\
&\quad \Delta(\mathbf{k})=2\Delta_0[\cos(k_x)+i\cos(k_y)]\ .
\end{aligned}
\tag{10}
$$

It is important to realize that none of these six cases are pure angular momentum eigenstates. For the antisymmetric cases [A, B, and C: $\Delta(-\mathbf{k})=-\Delta(\mathbf{k})$] the pairing states are superposition of odd angular momentum states. In these cases the quasiparticle excitation spectra can be written as

$$
\begin{aligned}
E_1(\mathbf{k})&=\sqrt{[|\mu|-|\gamma(\mathbf{k})|]^2+|\Delta(\mathbf{k})|^2}\ ,\\
E_2(\mathbf{k})&=\sqrt{[|\mu|+|\gamma(\mathbf{k})|]^2+|\Delta(\mathbf{k})|^2}\ .
\end{aligned}
\tag{11}
$$

It is evident that there will be nodes in the excitation spectrum at $k_x=-k_y$ and $k_x=k_y\pm\pi$ for case A, and at $k_x=k_y$ and at $k_x=-k_y\pm\pi$ for case B. Case C is in general nodeless.

For the symmetric cases [E, D and F; $\Delta(-\mathbf{k})=\Delta(\mathbf{k})$] the pairing states are a superposition of even angular momentum states. The quasiparticle excitation spectra are now

$$
\begin{aligned}
E_1(\mathbf{k})&=\big||\gamma(\mathbf{k})|-\sqrt{|\mu|^2+|\Delta(\mathbf{k})|^2}\big|\ ,\\
E_2(\mathbf{k})&=\big||\gamma(\mathbf{k})|+\sqrt{|\mu|^2+|\Delta(\mathbf{k})|^2}\big|\ .
\end{aligned}
\tag{12}
$$

Note that this form of excitation spectrum is different from the usual BCS form and it is always gapless. This feature is uniquely due to the spinless nature of the fermion.

We have performed a stability analysis of the superconducting state, with the normal state being either a simple tight binding or the $q=2$ flux phase, for all six symmetries listed in Eq. (10). The superconducting phases are found to be stable only for antisymmetric cases A, B, and C. Furthermore the competition is such that phase C is always the most stable, i.e., it has the lowest free energy [see Eq. (22) for the expression of the free energy]. Hence, numerical results are given only for this case in the remainder of the paper.

There are several important properties of phase C. First, it is nodeless; i.e., the quasiparticle excitation has a minimum gap. This is in contrast to the usual momentum-space pairing for which a spatial antisymmetric pairing state is always gapless. Second, it breaks the chiral symmetry due to the phase difference between the order parameters along the $\hat{x}$ and $\hat{y}$ directions. In addition, since the pairing order parameter carries finite angular momentum, both time-reversal and parity symmetries are broken in the superconducting state. This is in contrast to the normal state which does not break these symmetries in both the tight-binding and π staggered flux phase.[6] These two properties are similar to that of the Anderson-Brinkman-Morel (ABM) phase in the study of helium III.[11] Third, the gap order parameter is anisotropic in momentum space but the magnitude of the gap possesses the lattice symmetry. The experimental manifestations of these important properties require more studies.

If the normal state is the $q=2$ flux phase,[6] then phase C is closely related to the superconducting phase studied by Wang *et al.*[8] From Eq. (6) one finds

$$|\gamma(\mathbf{k})|^2=(2t)^2[\cos^2(k_x)+\cos^2(k_y)]$$

and

$$|\Delta(\mathbf{k})|^2=(2\Delta_0)^2[\sin^2(k_x)+\sin^2(k_y)]\ .$$

Therefore the gap is isotropic around the Fermi surface. Furthermore, from Eq. (10) one sees that the phase of the order parameter $\Delta(\mathbf{k})$ changes sign under the mirror reflection $k_y\rightarrow -k_y$. Hence the chirality of the order parameter at the Fermi surface pocket near the point $(\pi/2,\pi/2)$ is opposite to that near the point $(\pi/2,-\pi/2)$. This result is the same as that found by Wang *et al.*

Now let us turn to the quantitative solution for the case C. The coherence factors u, v as defined in (9) can be obtained analytically. They are

$$
\mathbf{u}=\begin{bmatrix}
\frac{1}{2}\sqrt{1+\xi_1} & \frac{1}{2}\sqrt{1+\xi_1}\,\dfrac{\gamma^*\mu}{|\gamma||\mu|}\\
\frac{1}{2}\sqrt{1+\xi_2} & -\frac{1}{2}\sqrt{1+\xi_2}\,\dfrac{\gamma^*\mu}{|\gamma||\mu|}
\end{bmatrix}
\tag{13}
$$

and

$$\mathbf{v}=\begin{bmatrix} \frac{1}{2}\sqrt{1-\xi_1}\,\dfrac{\Delta^*\gamma^*\mu}{|\Delta||\gamma||\mu|} & \frac{1}{2}\sqrt{1-\xi_1}\,\dfrac{\Delta^*}{|\Delta|} \\ -\frac{1}{2}\sqrt{1-\xi_2}\,\dfrac{\Delta^*\gamma^*\mu}{|\Delta||\gamma||\mu|} & \frac{1}{2}\sqrt{1-\xi_2}\,\dfrac{\Delta^*}{|\Delta|} \end{bmatrix}, \tag{14}$$

where

$$\xi_1(\mathbf{k})=-\mathrm{sgn}(\mu)\frac{|\mu|-|\gamma(\mathbf{k})|}{E_1(\mathbf{k})}\ ,$$
$$\xi_2(\mathbf{k})=-\mathrm{sgn}(\mu)\frac{|\mu|+|\gamma(\mathbf{k})|}{E_2(\mathbf{k})}\ , \tag{15}$$

with

$$\gamma(\mathbf{k})=2t[\cos(k_x)e^{i\Phi/4}+\cos(k_y)e^{-i\Phi/4}]\ ,$$
$$\Delta(\mathbf{k})=i2\Delta_0[\sin(k_x)+i\sin(k_y)]\ , \tag{16}$$

and the excitation spectrum $E_{1,2}(\mathbf{k})$ given by Eq. (11). Using these and equations (9) and (2) the self-consistent equation for the order parameter is

$$\begin{aligned}\frac{\Delta_{+\hat{x}}}{V}&=\langle A_i B_{i+\hat{x}}\rangle \\ &=\frac{1}{N}\sum_{\mathbf{k}}[u_{11}(\mathbf{k})v_{12}^*(\mathbf{k})+u_{21}(\mathbf{k})v_{22}^*(\mathbf{k})]e^{-ik_x}+\frac{1}{N}\sum_{\mathbf{k}}[u_{12}(-\mathbf{k})v_{11}^*(-\mathbf{k})-u_{11}(\mathbf{k})v_{12}^*(-\mathbf{k})]e^{-ik_x}n_1(\mathbf{k}) \\ &\quad+\frac{1}{N}\sum_{\mathbf{k}}[u_{22}(-\mathbf{k})v_{21}^*(-\mathbf{k})-u_{21}(\mathbf{k})v_{22}^*(-\mathbf{k})]e^{-ik_x}n_2(\mathbf{k}) \\ &=\frac{1}{N}\sum_{\mathbf{k}}\frac{\sin^2(k_x)}{2}\left[\frac{1-2n_1(\mathbf{k})}{E_1(\mathbf{k})}+\frac{1-2n_2(\mathbf{k})}{E_2(\mathbf{k})}\right]\Delta_{+\hat{x}}\end{aligned} \tag{17}$$

with similar equations for other components. Here $n_{1,2}=1/(e^{E_{1,2}/k_bT}+1)$ is the Fermi distribution function for the quasiparticles. Combining the equations for $\Delta_{+\hat{x}}$ and $\Delta_{+\hat{y}}$, the gap equation can be written in the symmetric form

$$\frac{1}{V}=\frac{1}{4N}\sum_{\mathbf{k}}\left[\frac{\tanh[E_1(\mathbf{k})/2k_bT]}{E_1(\mathbf{k})}+\frac{\tanh[E_2(\mathbf{k})/2k_bT]}{E_2(\mathbf{k})}\right]\times[\sin^2(k_x)+\sin^2(k_y)]\ . \tag{18}$$

The chemical potential is determined by fixing the total number of fermions per site δ which is

$$\begin{aligned}\delta&=\tfrac{1}{2}\langle A_i^\dagger A_i+B_i^\dagger B_i\rangle \\ &=\frac{1}{N}\sum_k[(u_{11}^2-v_{11}^2+u_{12}^2-v_{12}^2)n_1(\mathbf{k}) \\ &\quad+(u_{21}^2-v_{21}^2+u_{22}^2-v_{22}^2)n_2(\mathbf{k}) \\ &\quad+v_{11}^2+v_{12}^2+v_{21}^2+v_{22}^2]\ .\end{aligned} \tag{19}$$

Substituting Eqs. (13) and (14) results in

$$\delta=\frac{1}{2N}\sum_{\mathbf{k}}\left[1-\frac{1}{2}\xi_1(\mathbf{k})\tanh\left[\frac{E_1(\mathbf{k})}{2k_bT}\right]-\frac{1}{2}\xi_2(\mathbf{k})\tanh\left[\frac{E_2(\mathbf{k})}{2k_bT}\right]\right], \tag{20}$$

where $\xi_{1,2}(\mathbf{k})$ and $E_{1,2}(\mathbf{k})$ are given by Eqs. (15) and (11).

Equations (18) and (20) determine the gap and the chemical potential as functions of the temperature. The transition temperature T_c is given by setting $\Delta_0(T=0)=0$. In Fig. 2(a) we show the dependence of zero-temperature gap $\Delta_0(T=0)$ on the interaction V for both the tight-binding (TB) case and the flux phase (FP). In the small coupling region it has the BCS functional dependence $\Delta_0(T=0)\propto Ve^{-1/VN(\mu)}$.[12] The ratio of the gap to T_c, shown in Fig. 2(b), is found to be essentially independent of the coupling. For the flux phase, the gap is isotropic in the Fermi surface, the ratio $2|\Delta(T=0)|/T_c$ is about 3.6 [note $\Delta(\mathbf{k},T)$ is related to $\Delta_0(T)$ by Eq. (16)]. For the tight-binding case this ratio is anisotropic; the maximum is around 4. It is interesting to note that both values are close to the BCS value of 3.5; however, for the tight-binding case the minimum of this ratio could be much smaller.

It should be pointed out that the T_c which has been calculated here does not correspond to the transition temperature in the three-dimensional system. It is well known that in a pure 2D system the transition temperature is zero due to fluctuations. However, any 3D coupling will stabilize the 2D transition at a finite temperature, which depends on the mean-field transition temperature T_c calculated here.

Plotted in Fig. 3 is the temperature dependence of the order parameter $\Delta_0(T)$. The solid curve is the fit to the

BCS form

$$\Delta_0(T)=\Delta_0(0)\tanh(\alpha\sqrt{T_c/T-1}) \tag{21}$$

In both cases $\alpha=1.8$ is found to give an excellent fit.

The free energy per unit cell F_s is given by

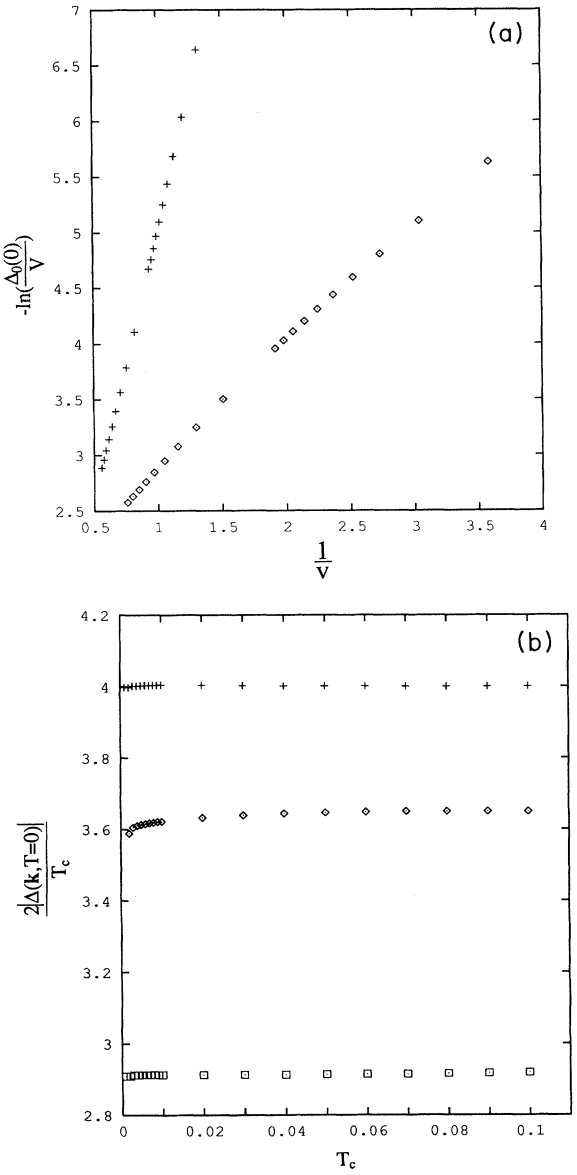

FIG. 2. (a) $-\ln[\Delta_0(0)/V]$ vs $1/V$ at $\delta=0.25$. A straight line indicates the weak coupling BCS dependence. The symbols are $\diamond$ for the flux phase and $+$ for the tight binding case. (b) The ratio $2|\Delta(\mathbf{k}, T=0)|/T_c$ at the Fermi surface with $\delta=0.25$ for various T_c. For flux phase the gap is isotropic on the Fermi surface and the ratio is close to that of BCS result of 3.5. For the tight-binding case the gap is anisotropic; the maximum and the minimum of the ratio are plotted. We found that the maximum of the ratio is insensitive to the change of chemical potential, while the minimum could be changed, dramatically reaching zero at $\delta=0.5$.

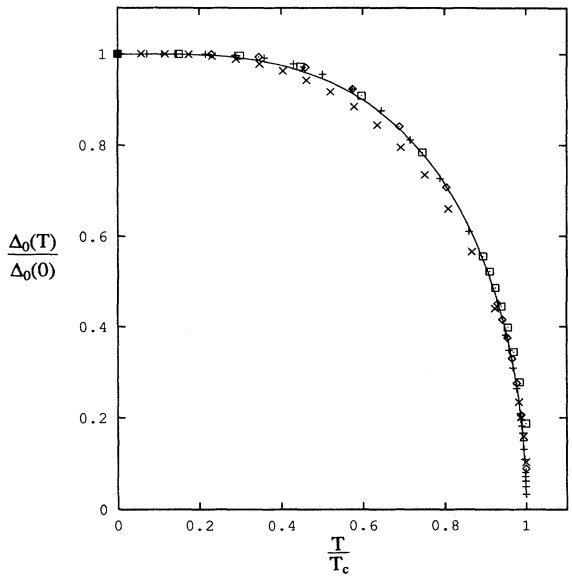

FIG. 3. $\Delta_0(T)/\Delta_0(0)$ vs T. The $\diamond$ and $+$ symbols are for the flux phase with the carrier density $\delta=0.25$ and the interactions $V=0.5t$ and $V=1.0t$, respectively. $\square$ and $\times$ denote the tight-binding nonflux phase with $V=1.0t$, and $\delta=0.25$, $\delta=0.45$, respectively. The solid line is the function $\tanh(\alpha\sqrt{T_c/T-1})$ with $\alpha=1.8$.

$$F_s-\mu(\Delta,T)\delta=-\frac{1}{2N}\sum_{\mathbf{k}}\left[E_1(\mathbf{k})\tanh\left[\frac{E_1(\mathbf{k})}{k_bT}\right]+E_2(\mathbf{k})\tanh\left[\frac{E_2(\mathbf{k})}{k_bT}\right]\right]+\frac{4\Delta_0^2}{V}-\mu(\Delta,t)-TS(T)\ , \tag{22}$$

where the entropy is

$$S(T)=-\frac{k_b}{N}\sum_{\mathbf{k},\,\alpha=1,2}\{n_\alpha(\mathbf{k})\ln n_\alpha(\mathbf{k})+[1-n_\alpha(\mathbf{k})]\ln[1-n_\alpha(\mathbf{k})]\}\ . \tag{23}$$

Note that both the chemical potential μ and the gap $\Delta_0(T)$ are self-consistently determined by Eqs. (20) and (18) given the coupling V, the number of fermions per site δ, and the temperature T. We have calculated the free energy at several different dopings for all six cases listed in Eq. (10). It is found that only the superconducting states with antisymmetric order parameter have lower free energy than that of the normal state at the same temperature. Furthermore, in the superconducting state, phase C always has the lowest free energy.

The bulk critical magnetic field $H_c(T)$ is determined from

$$\frac{H_c^2(T)}{8\pi}=F_n(T)-F_s(T)\ , \tag{24}$$

where $F_n(T)$ is the normal-state energy at the same tem-

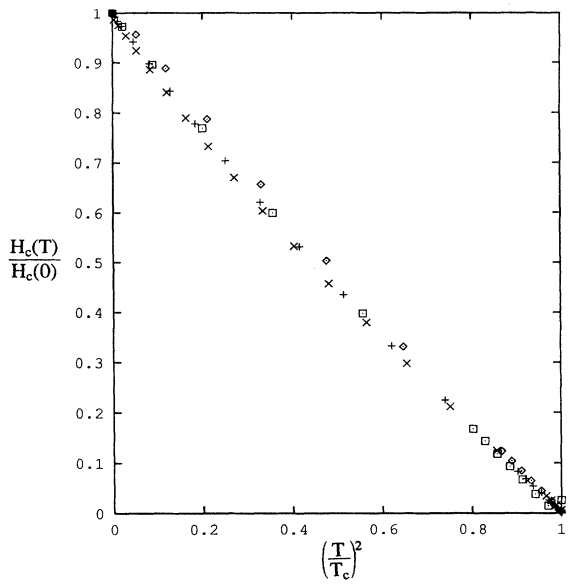

FIG. 4. The bulk critical field H_c [defined in Eq. (24)] plotted against $(T/T_c)^2$. A straight line would be the result of a two-fluid model. The symbols in the figure have the same meaning as in Fig. 3.

perature. In Fig. 4 we show the temperature dependence of $H_c(T)$. Again it is found that the result is very similar to that of the BCS solution.[12]

In conclusion, we have studied the real-space pairing instabilities of spinless fermions on a two-dimensional square lattice. Motivated by our earlier semiclassical calculations of the t-J model, both no-flux tight binding and flux phase were studied. In both cases we found that the most stable pairing state breaks both the time-reversal and parity symmetries. Such a pairing state is not in contradiction with recent optical experiments on the high-T_c oxide superconductors, which indicate such symmetries may be broken.[13] However, there may also be additional observable effects, such as orbital ferromagnetism due to the finite angular momentum of the pairing state, similar to what has been observed in helium III.[14] Further studies are needed to quantitatively estimate such effects.

The quasiparticle excitation in the tight-binding case is found to be anisotropic and to possess a minimum gap which may be much smaller than the maximum gap. The results for the π staggered flux phase are in qualitative agreement with earlier meanfield analysis. Though the real-space pairing state is a superposition of many angular momentum eigenstates, the gap $\Delta_0(T)$, T_c, and the critical field H_c are all found to be similar to those of the classical BCS solutions for the momentum-space pairing. Combination of these effects may lead to some unusual thermodynamical properties in the superconducting state, such as the absence of or weak Hebel-Slichter peak in the nuclear relaxation rate and a finite density of states for the energy smaller than the maximum gap.

J.P.L. is indebted to A. Leggett, R. Martin, and V. Kalmeyer for useful discussions. The research at University of Illinois is supported by Grant No. NSF-STC-8809854 through the Science and Technology Center for Superconductivity.

[1]P. W. Anderson, Science **235**, 1196 (1987).
[2]F. C. Zhang and T. M. Rice, Phys. Rev. B **37**, 3759 (1988).
[3]B. I. Shraiman and E. D. Siggia, Phys. Rev. Lett. **62**, 1564 (1989).
[4]C. L. Kane, P. A. Lee, T. K. Ng, B. Chakraborty, and N. Read, Phys. Rev. B **41**, 2653 (1990); B. Chakraborty, N. Read, C. L. Kane, and P. A. Lee, *ibid.* **42**, 4819 (1990).
[5]I. Affleck and J. B. Marston, Phys. Rev. B **37**, 3774 (1988).
[6]W. Barford and Jian Ping Lu, Phys. Rev. B **43**, 3540 (1991).
[7]M. Grilli and G. Kotliar, Phys. Rev. Lett. **64**, 1170 (1990).
[8]Z. Wang, G. Kotliar, and X. F. Wang, Phys. Rev. B **42**, 8690 (1990).
[9]G. J. Chen, R. Joynt, F. C. Zhang, and C. Gross, Phys. Rev. B **42**, 2662 (1990).
[10]For a recent review on the order-parameter symmetry in high-T_c superconductors, see J. Annett, N. Goldenfeld, and S. Renn, in *Physical Properties of High Temperature Superconductors II,* edited by D. Ginsberg (World Scientific, Singapore, 1990).
[11]A. J. Leggett, Rev. Mod. Phys. **47**, 331 (1975).
[12]J. R. Schrieffer, *Theory of Superconductivity* (Addison-Wesley, New York, 1983).
[13]K. Kiefl *et al.*, Phys. Rev. Lett. **64**, 2082 (1990); K. Lyons *et al.*, *ibid.* **64**, 2949 (1990); S. Spielman *et al.*, *ibid.* **65**, 123 (1990).
[14]A. J. Leggett, Nature **270**, 585 (1977); D. N. Paulson and J. C. Wheatley, Phys. Rev. Lett. **40**, 577 (1978).